Inorg. Chem. **2008**, *47*, 9419−9430

Iron(III) Uptake and Release by Chrysobactin, a Siderophore of the Phytophatogenic Bacterium *Erwinia chrysanthemi*

Vladislav Tomišić,[†] Sylvie Blanc,[†] Mourad Elhabiri,[†] Dominique Expert,*[,‡] and Anne-Marie Albrecht-Gary*[,†]

Laboratoire de Physico-Chimie Bioinorganique, ULP-CNRS (UMR 7177), Institut de Chimie, ECPM, 25 rue Becquerel, 67200 Strasbourg, France, and Laboratoire Interactions Plantes-Pathogènes, INRA/INA-PG/UPMC (UMR 217), 16 rue Claude Bernard, 75231 Paris Cedex 05, France

Received June 20, 2008

The plant pathogenic enterobacterium *Erwinia chrysanthemi* causes important soft-rot disease on a wide range of plants including vegetables and ornamentals of economic importance. It produces a major mono(catecholate) siderophore, chrysobactin (α-*N*-(2,3-dihydroxybenzoyl)-D-lysyl-L-serine). To unravel the role of chrysobactin in the virulence of *E. chrysanthemi*, its iron(III) coordination properties were thus investigated in aqueous solutions using electrospray ionization mass spectrometric, potentiometric, and spectrophotometric methods. Moreover, kinetic experiments allowed us to determine the uptake and release mechanisms. The formation mechanism of the 1:1 complex reveals a key role of the terminal carboxylic group of chrysobactin in the binding of either $FeOH^{2+}$ or $Fe_2(OH)_2^{4+}$. The proton-driven dissociation of the ferric tris-, bis-, and mono(chrysobactin) complexes was also studied. For these three ferric complexes, a single protonation triggers the release of the bound chrysobactin molecule. Interestingly, the dissociation of the last ligand proceeded via the formation of an intermediate for which a salicylate-type mode of bonding was proposed.

Introduction

Under iron-deficient conditions, almost all microorganisms excrete highly efficient and specific ferric ion chelators, termed siderophores.[1−3] These molecules typically possess hydroxamate, catecholate, and/or α-hydroxycarboxylate ligating groups. Although many siderophores are hexadentate ligands, several natural iron sequestering agents of lower denticity have been described,[4] and their iron(III) complexation properties were thoroughly studied.[5,6] One of them is chrysobactin (noted Cb), α-*N*-(2,3-dihydroxybenzoyl)-D-lysyl-L-serine (Figure 1), a mono(catecholate) siderophore first isolated by Persmark et al.[7] from the plant pathogenic enterobacterium *Erwinia chrysanthemi*, which causes soft-rot disease on a wide range of plants including vegetables and ornamentals of economic importance.

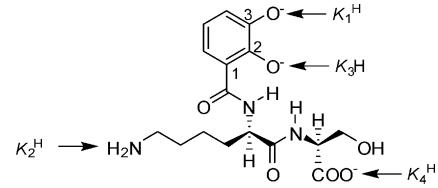

Figure 1. Structure of fully deprotonated chrysobactin and attribution of the protonation sites.

More recently, chrysobactin was shown to be produced by several strains of *E. carotovora subsp. carotovora* deleterious to potato plants.[8]

* To whom correspondence should be addressed. E-mail: amalbre@chimie.u-strasbg.fr (A.-M.A.-G.), Dominique.Expert@inapg.inra.fr (D.E.).
† ULP-CNRS (UMR 7177), Institut de Chimie.
‡ INRA/INA-PG/UPMC (UMR 217).

(1) Neilands, J. B. *Struct. Bonding (Berlin)* **1984**, *58*, 1–24.
(2) Raymond, K. N.; Müller, G.; Matzanke, B. F. *Top. Curr. Chem.* **1984**, *123*, 49–102.
(3) Winkelmann, G. *CRC Handbook of Microbial Iron Chelates*; CRC Press: Boca Raton, FL, 1991; pp 15−64.
(4) (a) Albrecht-Gary, A. M.; Crumbliss, A. L. In *Metal Ions in Biological Systems*; Sigel A., Siegel H. Eds.; Marcel Dekker, Inc.: New York, 1998; pp 239−327, and references cited therein. (b) Albrecht-Gary, A. M., Crumbliss, A. L. *Scientific Bridges for 2000 and Beyond,* TEC & DOC Editions, Académie des Sciences; Institut de France: Paris, 1999; pp 73−89.
(5) Telford, J. R.; Raymond, K. N. *Inorg. Chem.* **1998**, *37*, 4578–4583.
(6) Boukhalfa, H.; Brickman, T. J.; Armstrong, S. K.; Crumbliss, A. L. *Inorg. Chem.* **2000**, *39*, 5591–5602.
(7) Persmark, M.; Expert, D.; Neilands, J. B. *J. Biol. Chem.* **1989**, *264*, 3187–3193.
(8) Barnes, H. H.; Ishimaru, C. A. *Biometals* **1999**, *12*, 83–87.

10.1021/ic801143e CCC: $40.75
Published on Web 09/20/2008

The role of chrysobactin in the virulence of *E. chrysanthemi* is well documented. *E. chrysanthemi* mutants altered in the biosynthesis of chrysobactin produce only localized symptoms on African violets or *Arabidopsis* plants, and their growth in planta is reduced compared to a chrysobactin-proficient strain.[9−11] Chrysobactin was detected in leaf intercellular fluids from infected plants,[12] and as a catechol-type siderophore, it is expected to readily compete with plant iron ligands such as citrate or other organic acids present in the apoplasm.[13] Indeed, chrysobactin-like enterobactin can remove iron(III) from EDDHA, a powerful ferric ion complexing ligand[14] (pFe = 25.0 at pH 6.5), which is not the case of achromobactin (Figure S1 in the Supporting Information), a second siderophore synthesized by *E. chrysanthemi*.[10] More recently, it was reported that chrysobactin, unlike its ferric complex, can activate a defense response from the host plant, leading to elevated levels of ferritins.[11]

Ferric chrysobactin is transported back into the bacterial cell via its specific TonB-dependent outer membrane receptor Fct and a cytoplasmic membrane permease.[15−19] Moreover, ferric enterobactin is used as an exogenous iron carrier by *E. chrysanthemi* cells, and its transport occurs via another TonB-dependent receptor immunologically related to the *Escherichia coli* ferric Enterobactin receptor FepA.[17] On the other hand, the same permease mediates the transport of the ferric complexes of these two siderophores, indicating a low specificity for the passage of these chelates through the cytoplasmic membrane. Once inside the cytosol, ferric chrysobactin releases its iron, and the ligand is degraded by a specific peptidase.[18] It was proposed that the action of this peptidase prevents the bacterial cells from being intracellularly iron depleted by chrysobactin.

In order to further understand the biological role of chrysobactin, as well as its interaction with its membrane receptor, we conducted a detailed analysis of the physicochemical properties of this siderophore. Chrysobactin belongs to a class of siderophores that are basically dihydroxybenzoic acid derivatives (Figure 1) of amino acids or peptides.[7,19,20] Using NMR analysis of the gallium(III) chrysobactin complex, Persmark and Neilands[19] have shown that only the catecholate group is involved in the chelation. Depending on the pH and the metal/ligand concentration ratio, chrysobactin was found to form ferric complexes of different stoichiometries, from 1:1 to 1:3 (Fe/Cb).[19] It was also shown that when the ligand was in excess (≥ 4), a mixture of ferric bis- and tris(chrysobactin) complexes was present in solution at physiological pH.[19] The aim of the present work is to determine the stability constants of the ferric complexes in order to assess the affinity of chrysobactin for iron(III). We report here the results of detailed potentiometric and spectrophotometric investigations on iron(III) complexation by chrysobactin, as well as on the protonation of the free ligand. In order to gain insight into the mechanistic features of iron uptake and release by chrysobactin, studies of the formation and dissociation kinetics of the ferric chrysobactin complexes were carried out.

Experimental Section

Materials. All of the solutions were prepared in water. All of the stock solutions were prepared by weighing solid products using an AG 245 Mettler Toledo analytical balance (precision 0.01 mg). Distilled water was further purified by passing through a mixed bed of ion exchangers (Bioblock Scientific R3-83002 and M3-83006) and activated carbon (Bioblock Scientific ORC-83005). Distilled water was also deoxygenated using CO_2- and O_2-free argon prior to use (Sigma Oxiclear cartridge). Iron(III) perchlorate stock solutions ($\sim 10^{-2}$ M) were prepared immediately before use by dissolving an appropriate amount of solid ferric perchlorate [$Fe(ClO_4)_3 \cdot 9H_2O$, Fluka, pract.] in a $HClO_4$ solution (Merck, suprapur). The iron(III) concentrations were ascertained by back-titration with thorium nitrate (Merck, p.a.) in an excess of a standardized Na_2H_2EDTA solution (Merck, Titriplex III) and xylenol orange as an indicator.[21] The glassware used was rinsed after each experiment with a hydrochloric acid solution to remove all traces of iron. Chrysobactin was synthesized according to the described procedure.[7] The solutions of the ligand were prepared by dissolution of the solid sample, and their concentrations were checked by spectrophotometry ($\varepsilon_{318} = 3000$ M^{-1} cm^{-1} at p[H] = 6.5).[7]

Electrospray Ionization Mass Spectrometric Measurements. The electrospray ionization mass spectra (ESI-MS) of solutions of free chrysobactin ($[Cb]_{tot} = 1.0 \times 10^{-4}$ M, p[H] = 6.5, 50 mM ammonium formate (Aldrich)) and its ferric complexes ($[Cb]_{tot} = 4.0 \times 10^{-4}$ M, $[Fe^{III}]_{tot} = 1.0 \times 10^{-4}$ M; p[H] = 5.1, 24 mM triethylamine (SDS), 30 mM acetic acid (Fluka), and p[H] = 10.4, 50 mM triethylamine (SDS), 31 mM hydrochloric acid (Merck)) were obtained with a VG BioQ triple-quadrupole spectrometer (Micromass, Altrincham, U.K.) operating in the positive ion mode (ESI-MS^+). The samples were continuously introduced into the mass spectrometer source with a syringe pump (Harvard type 55 1111; Harvard Apparatus Inc., South Natick, MA) at a flow rate of 5−10 μL min^{-1}. For ESI, the source temperature was set at 80 °C and the sampling cone voltage was set at 50 V. The calibration of the instrument was performed using signals of multiprotonated ions from horse myoglobin (Sigma). Several spectra of each investigated sample were recorded and averaged to obtain the final spectrum.

Potentiometric Titrations. The titrations were performed in a jacketed cell maintained at 25.0(2) °C by means of a constant-temperature water circulation bath (Haake FJ). The solutions were continuously deoxygenated by bubbling with oxygen-free argon. The free hydrogen ion concentrations were measured with a

(9) Masclaux, C.; Expert, D. *Plant J.* **1995**, *7*, 121–128.
(10) Franza, T.; Mahe, B.; Expert, D. *Mol. Macrobiol.* **2005**, *55*, 261–275.
(11) Dellagi, A.; Rigault, M.; Segond, D.; Roux, C.; Kraepiel, Y.; Cellier, F.; Briart, J. F.; Gaymard, F.; Expert, D. *Plant J.* **2005**, *43*, 262–272.
(12) Neema, C.; Laulhere, J. P.; Expert, D. *Plant Physiol.* **1993**, *102*, 967–973.
(13) Brown, J. C. *Plant Cell Environ.* **1978**, *1*, 249–257.
(14) Sierra, M. A.; Gomez-Gallego, M.; Alcazar, R.; Lucena, J. L.; Yuanta, F.; Garcia-Marco, S. *Dalton Trans.* **2004**, 3741–3747.
(15) Sauvage, C.; Franza, T.; Expert, D. *J. Bacteriol.* **1996**, *178*, 1227–1231.
(16) Enard, C.; Expert, D. *Microbiol.* **2000**, *146*, 2051–2058.
(17) (a) Enard, C.; Diolez, A.; Expert, D. *Plant Soil* **1991**, *130*, 263–271. (b) Buchanan, S. K.; Smith, B. S.; Venkatramani, L.; Xia, D.; Esser, L.; Palnitkar, M.; Chakraborty, R.; van der Helm, D.; Deisenhofer, J. *Nat. Struct. Biol.* **1999**, *6*, 56–63.
(18) Rauscher, L.; Expert, D.; Matzanke, B. F.; Trautwein, A. *J. Biol. Chem.* **2002**, *277*, 2385–2395.
(19) Persmark, M.; Neilands, J. B. *Biometals* **1992**, *5*, 29–36.
(20) Persmark, M.; Expert, D.; Neilands, J. B. *J. Bacteriol.* **1992**, *174*, 4783–4789.
(21) *Méthodes d'analyses complexométriques avec les Titriplex*; Merck: Darmstadt, Germany, 1990; p 45.

combined glass−Ag/AgCl microelectrode (Ingold, High Alkalinity) and a Tacussel Isis 20000 millivoltmeter. The electrode was calibrated to read hydrogen ion concentrations by titration of a $HClO_4$ (Merck, suprapure) solution, previously standardized by colorimetric titration with sodium borate decahydrate ($Na_2B_4O_7 \cdot 10H_20$, puriss. p.a., ACS, Fluka) and methyl red as an indicator,[21] with a CO_2-free NaOH (Carlo Erba, p.a.) solution, previously standardized by colorimetric titration with potassium hydrogen phthalate (puriss. p.a., Fluka) and phenolphthalein as an indicator.[21] The GLEE program[22] was applied for the glass electrode calibration and allowed us to check the carbonate percentage in the NaOH solution used. The ionic strength was fixed at $I = 0.1$ M with sodium perchlorate (Merck, p.a.). ***Caution!*** *Perchlorate salts combined with organic ligands are potentially explosive and should be handled in small quantities and with the necessary precautions*.[23] The potentiometric titrations of the free ligand ($[Cb]_{tot} = 7.3 \times 10^{-4}$ M) and its ferric complexes ($[Fe^{III}]_{tot} = 2.06 \times 10^{-4}$ M, $[Cb]_{tot} = 6.9 \times 10^{-4}$ M; Figure 2) were carried out by the addition of known volumes of standardized NaOH (0.1 M, Carlo Erba, p.a.) or $HClO_4$ (0.1 M, Merck, suprapur) with a piston microburette (Gilmont). The potentiometric data (about 200 points collected over the pH range 3.5−11.0) were refined with the Hyperquad 2000 program, which uses a nonlinear least-squares method.[24]

The potentiometric titration of the ferric chrysobactin complexes ($[Fe^{III}]_{tot}/[Cb]_{tot} = 1/3.3$; starting p[H] = 10.20) with perchloric acid is shown in Figure 2. Two inflections can be observed: a first one at $a = 2$ (a stands for moles of acid added per mole of metal) and p[H] ∼ 8 and the second one at $a = 4$ and p[H] ∼ 5. The part of the titration curve from $a = 0$ to 2 implied two successive protonations of the tris(chrysobactin)iron(III) complex [wine-red color typical for tris(catecholate)iron(III) species]. Between $a = 2$ and 4, tris(chrysobactin)iron(III) dissociates to the bis(chrysobactin)iron(III) complex [blue-violet color typical for bis(catecholato)iron(III) species]. From $a = 4$ to 5, a protonation of the bis(chrysobactin)iron(III) complex takes place.

Potentiometric and Spectrophotometric Titrations. The spectrophotometric titration versus p[H] of ferric chrysobactin complexes was performed in two sets of experiments. It was indeed observed that the formation of a ferric mono(chrysobactin) complex under acidic conditions (p[H] < 4) was followed by a redox reaction [a qualitative colorimetric test with 2,2′-dipyridyl evidenced the presence of iron(II)], which led to the degradation of the ferric complex. Such redox reactions have already been observed for various ferric mono(catecholate) complexes.[25,26] Therefore, a classical spectrophotometric titration could not be used to determine the stability constants of the species under acidic conditions. To overcome that problem, a stopped-flow spectrophotometer equipped with a diode-array detector (Applied Photophysics SX-18MV) was used to obtain the absorption spectra at p[H] = 2.00 before the subsequent much slower redox reaction took place. Solutions of iron(III) (concentrations ranging from 9.00×10^{-5} to 4.97×10^{-3} M) and chrysobactin (1.5×10^{-4} M) were mixed by means of a stopped-flow device, and a series of 400 spectra per run were recorded as a function of time. The final equilibrium spectrum was obtained as an average of six spectra taken (at equilibrium) from two runs. Special care was taken to ensure that complete equilibration was attained. Spectrophotometric titration of the solution with $[Cb]_{tot} = 3.3 \times 10^{-4}$ M and $[Fe^{III}]_{tot} = 7.89 \times 10^{-5}$ M (Figure 3) was also performed in the p[H] range from 9.40 to 4.07. The p[H] was first increased by the addition of standardized NaOH, and the solution was then titrated with standardized $HClO_4$. After the p[H] was stabilized, an aliquot of the solution was taken, and its visible absorption spectrum (400−800 nm) was recorded using a Kontron Uvikon 941 spectrophotometer maintained at 25.0(2) °C by the flow of a Haake FJ thermostat. Optical quartz cells of 1.0 cm path length were used, and the sampling interval was set at 1 nm with an integration time of 0.3 s. The spectrophotometric data were processed[27] with the Specfit program, which adjusts the stability constants and the corresponding molar extinction coefficients (M^{-1} cm^{-1}) of the species at equilibrium. Specfit[28−30] uses factor analysis to reduce the absorbance matrix and to extract the eigenvalues prior to the multiwavelength fit of the reduced data set according to the Marquardt algorithm.[31,32] Distribution curves of the various species were calculated using the Haltafall program.[33]

Kinetic Measurements. The formation kinetics of ferric mono(chrysobactin) complex was studied under pseudo-first-order conditions with respect to Cb at 680 nm. $[Cb]_{tot}$ was 1.4×10^{-4} M, while $[Fe^{III}]_{tot}$ varied from 1.50×10^{-3} to 5.00×10^{-3} M. The solutions were prepared in a $HClO_4/NaClO_4$ medium to obtain a constant ionic strength of 0.1 M and p[H] values ranging from 1.70 to 2.05. The course of the formation reaction was monitored at 25.0(2) °C by means of an Applied Photophysics SX-18MV stopped-flow spectrophotometer.

Proton-promoted dissociation kinetics of ferric tris-, bis-, and mono(chrysobactin) complexes were studied separately at 1.0 M ionic strength ($NaClO_4/HClO_4$) and 25.0(2) °C using a stopped-flow spectrophotometer (Applied Photophysics SX-18MV). The decay of absorbance as a function of time was monitored at wavelengths corresponding to the maxima of charge-transfer absorption bands of the respective complexes. Parallel experiments were also carried out using a diode-array detector.

The dissociation reaction of the ferric tris(chrysobactin) complex was studied by mixing of an iron(III) (1.49×10^{-4} M) and chrysobactin (5.9×10^{-4} M) solution at p[H] = 8.56 with an equal volume of a solution of 50 mM of 2-morpholinoethanesulfonic acid (MES; Aldrich) buffer adjusted to the desired p[H] (4.80−6.40). The ionic strength was fixed at 1.0 M ($NaClO_4$) in all of the solutions. The dissociation of the red tris(chrysobactin) complex was monitored at 493 nm [$\lambda^{max}(Fe(Cb)_3)$]. A single exponential decrease of absorbance versus time was observed with no loss of the spectrophotometric signal during the mixing time (∼3 ms) of the fast-mixing device. It is noteworthy that the variation of the total MES concentration between 10 and 100 mM had no effect on the observed dissociation kinetics.

The dissociation of the ferric bis(chrysobactin) complex was followed at 572 nm [$\lambda^{max}(Fe(Cb)_2)$] by mixing of an iron(III)

(22) Gans, P.; O'Sullivan, B. *GLEE 3.0.15*; Protonic Softwares: Leeds, U.K., and Berkeley, CA, 2005. (b) Gans, P.; O'Sullivan, B. *Talanta* **2000**, *51*, 33–37.
(23) (a) Wolsey, W. C. *J. Chem. Educ.* **1978**, *55*, A355–A337. (b) Raymond, K. N. *Chem. Eng. News* **1983**, *61*, 4.
(24) (a) Gans, P.; Sabatini, A.; Vacca, A. *HYPERQUAD 2000*, version 2.1: Leeds, U.K., and Florence, Italy, 2000. (b) Gans, P.; Sabatini, A.; Vacca, A. *Talanta* **1996**, *43*, 1739–1753.
(25) Mentasti, E.; Pelizzetti, E.; Saini, G. *J. Chem. Soc., Dalton Trans.* **1973**, 2609–2614.
(26) Xu, J.; Jordan, R. B. *Inorg. Chem.* **1988**, *27*, 4563–4566.
(27) Rossoti, F. J. C.; Rossoti, H. S.; Whewell, R. J. *J. Inorg. Nucl. Chem.* **1971**, *33*, 2051–2065.
(28) Gampp, H.; Maeder, M.; Meyer, C. J.; Zuberbühler, A. D. *Talanta* **1985**, *32*, 95–101.
(29) Gampp, H.; Maeder, M.; Meyer, C. J.; Zuberbühler, A. D. *Talanta* **1985**, *32*, 257–264.
(30) Gampp, H.; Maeder, M.; Meyer, C. J.; Zuberbühler, A. D. *Talanta* **1986**, *33*, 943–951.
(31) Marquardt, D. W. *J. Soc. Ind. Appl. Math.* **1963**, *11*, 431–441.
(32) Maeder, M.; Zuberbühler, A. D. *Anal. Chem.* **1990**, *62*, 2220–2224.
(33) Ingri, N.; Kakolowicz, W.; Sillen, L. G.; Warnqvist, B. *Talanta* **1967**, *14*, 1261–1286.

(2.04×10^{-4} M) and chrysobactin (4.1×10^{-4} M) solution at p[H] = 6.40 with an equal volume of a solution of 50 mM formate buffer adjusted to the desired p[H] (2.55−3.55). The ionic strength was fixed at 1.0 M ($NaClO_4$) in all of the solutions. A single-exponential decay of absorbance versus time was recorded. Importantly, the variation of the total formate concentration between 10 and 100 mM did not influence the dissociation kinetics.

Because the preparation of the ferric mono(chrysobactin) complex was precluded because of the intramolecular redox reaction, the dissociation of the ferric bis(chrysobactin) complex was thus studied by mixing of an iron(III) (1.59×10^{-4} M) and chrysobactin (3.2×10^{-4} M) solution at p[H] = 6.32 with an equal volume of $HClO_4/NaClO_4$ solutions to give the desired p[H]. In this set of experiments, the $[H^+]$ range was 0.010−0.50 M. Under these experimental conditions, the ferric bis(chrysobactin) complex rapidly released one ligand, leading to the ferric mono(chrysobactin) complex whose dissociation was thus followed either at 680 nm or by use of a diode-array detector. For the diode-array experiments, the concentrations were $[Fe^{III}]_{tot} = 2.33 \times 10^{-4}$ M and $[Cb]_{tot} = 4.7 \times 10^{-4}$ M.

The data sets, averaged out of at least three replicates, were recorded and analyzed with the commercial software Biokine.[34] This program fits up to three exponential functions to the experimental curves using the Simplex algorithm[35] after initialization with the Padé−Laplace method.[36] Origin 5.0 was used to process kinetic data.[37]

Results

Acido−Basic Properties of Free Chrysobactin. The variation of p[H] during the potentiometric titration of the free chrysobactin is given in Figure S4 in the Supporting Information. Three well-separated buffer regions were observed. An attempt to determine the highest protonation constant of chrysobactin, i.e., the one of the hydroxyl in the meta-position to the amide linkage (Figure 1), was not successful, probably because of the decomposition of the ligand at very high p[H] (the same was observed with some analogue catecholate ligands[38,39]). As an estimation, the first protonation constant of *N*,*N*-dimethyl-2,3-dihydroxybenzamide (DMB), determined previously as $\log K_1^H = 12.1$,[38] was used throughout this study. The processing of the potentiometric data allowed us to determine three stepwise protonation constants. Their values are given in Table 1 together with those obtained from spectrophotometric versus pH titration. Distribution diagrams of the protonated species of chrysobactin are given in Figure S5 in the Supporting Information.

Stoichiometry of the Ferric Chrysobactin Complexes. The use of ESI-MS to determine the stoichiometry of metallic complexes in solution is well documented[40,41] and has been employed by us for this purpose on previous occasions.[42−46] ESI-MS of the free chrysobactin gave, in the positive detection mode, peaks at *m*/*z* 370.3 and 739.4, which correspond to $[CbH_4]^+$ and $[Cb_2H_7]^+$ ions, respectively, where Cb stands for the fully deprotonated ligand (Figure S2 in the Supporting Information). These results are in very good agreement with fast atom bombardment MS results published by Persmark et al.[7] under the same experimental conditions. Ferric chrysobactin complexes gave peaks at *m*/*z* 792.2 and 1161.4, which correspond to $[FeCb_2H_4]^+$ and $[FeCb_3H_7]^+$ species, respectively (Figure S3 in the Supporting Information).

Table 1. Successive Protonation Constants[a] of Free Chrysobactin and Global Stability Constants[b] of Ferric Chrysobactin Complexes[c]

	potentiometry	spectrophotometry
$\log K_1^H$	12.1[d]	
$\log K_2^H$	10.61(1)	
$\log K_3^H$	6.73(1)	
$\log K_4^H$	3.17(1)	
$\log \beta_{FeCbH_2}$		33.1(1)
$\log \beta_{FeCb_2H_2}$	51.93(6)	52.1(3)
$\log \beta_{FeCb_2H_3}$	56.29(9)	
$\log \beta_{FeCb_3H}$	50.77(9)	
$\log \beta_{FeCb_3H_2}$	62.03(6)	
$\log \beta_{FeCb_3H_3}$	72.13(6)	72.5(3)

[a] Successive protonation constants: $LH_{n-1}^{n-4} + H^+ \rightleftarrows LH_n^{n-3}$. [b] Global stability constant: $Fe^{3+} + lCb^{3-} + hH^+ \rightleftarrows FeCb_lH_h^{3(l-1)+h}$. Estimated errors = 3σ. [c] Solvent = water; $I = 0.1$ M ($NaClO_4$); $T = 25.0(2)$ °C. [d] $\log K_1^H = 12.1$ estimated from DMB.[38]

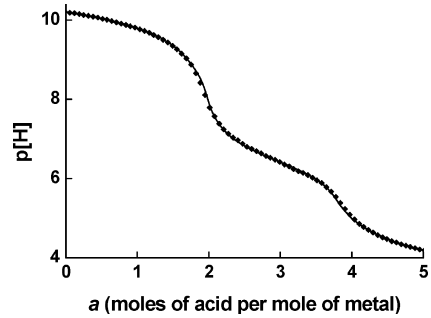

Figure 2. Potentiometric titration curve of ferric chrysobactin. $[Cb]_{tot} = 6.9 \times 10^{-4}$ M; $[Fe^{III}]_{tot} = 2.06 \times 10^{-4}$ M; solvent = water; $I = 0.1$ M ($NaClO_4$); $T = 25.0(2)$ °C. Each second point is shown; the solid line corresponds to the calculated fit.

Stability of the Ferric Chrysobactin Complexes. Two ferric chrysobactin complexes, bis- and tris(chelate)iron(III) species, respectively, have been characterized by potentiometric titrations between p[H] = 4 and 10, as well as their protonated forms (Figure 2).

The corresponding stability constants are given in Table 1. Moreover, in order to examine ferric mono(chelate)

(34) Bio-Logic Company, Ed. Bio-Logic Company, Echirolles, 1991.
(35) Nelder, J. A.; Mead, R. *Comput. J.* **1965**, *7*, 308–313.
(36) Yeramian, E.; Claverie, P. *Nature* **1987**, *326*, 169–174.
(37) Microcal Software, Inc., Northampton, MA, 1991−1997.
(38) Harris, W. R.; Carrano, C. J.; Cooper, S. R.; Sofen, S. R.; Avdeef, A. E.; McArdle, J. V.; Raymond, K. N. *J. Am. Chem. Soc.* **1979**, *101*, 6097–6104.
(39) Loomis, L. D.; Raymond, K. N. *Inorg. Chem.* **1991**, *30*, 906–911.
(40) Piguet, C.; Bernardinelli, G.; Hopfgartner, G. *Chem. Rev.* **1997**, *97*, 2005–2062.
(41) (a) Hopfgartner, G.; Piguet, C.; Henion, J. D.; Williams, A. F. *Helv. Chim. Acta* **1993**, *76*, 1759–1766. (b) Hopfgartner, G.; Piguet, C.; Henion, J. D. *J. Am. Soc. Mass Spectrom.* **1994**, *5*, 748–756.
(42) Blanc, S.; Yakirevitch, P.; Leize, E.; Meyer, M.; Libman, J.; Van Dorsselaer, A.; Albrecht-Gary, A. M.; Shanzer, A. *J. Am. Chem. Soc.* **1997**, *119*, 4934–4944.
(43) Fatin-Rouge, N.; Blanc, S.; Leize, E.; Van Dorsselaer, A.; Baret, P.; Pierre, J. L.; Albrecht-Gary, A. M. *Inorg. Chem.* **2000**, *39*, 5771–5778.
(44) Fatin-Rouge, N.; Blanc, S.; Pfeil, A.; Rigault, A.; Albrecht-Gary, A. M.; Lehn, J. M. *Helv. Chim. Acta* **2001**, *84*, 1694–1711.
(45) Stein Martins, G. T.; Szpoganicz, B.; Tomisic, V.; Humbert, N.; Elhabiri, M.; Albrecht-Gary, A. M.; Sala, L. F. *Inorg. Chim. Acta* **2004**, *357*, 2261–2268.
(46) (a) Hamacek, J.; Blanc, S.; Elhabiri, M.; Leize, E.; Van Dorsselaer, A.; Piguet, C.; Albrecht-Gary, A. M. *J. Am. Chem. Soc.* **2003**, *125*, 1541–1550. (b) Elhabiri, M.; Hamacek, J.; Bünzli, J.-C. G.; Albrecht-Gary, A. M. *Eur. J. Inorg. Chem.* **2004**, 51–62.

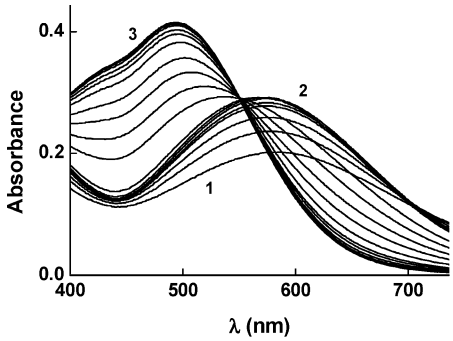

Figure 3. Visible spectra (corrected for dilution) of ferric chrysobactin complexes, recorded as a function of p[H]. $[Cb]_{tot} = 3.3 \times 10^{-4}$ M; $[Fe^{III}]_{tot} = 7.89 \times 10^{-5}$ M; $l = 1$ cm; solvent = water; $I = 0.1$ M ($NaClO_4$); $T = 25.0(2)$ °C; p[H] = 4.07 (**1**), 5.66 (**2**), and 9.40 (**3**).

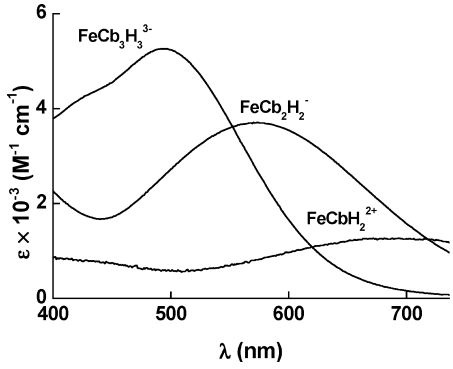

Figure 4. Calculated electronic spectra of ferric chrysobactin complexes.

chrysobactin, we carried out spectrophotometric titration at p[H] = 2.00 using a stopped-flow technique, in order to separate the slow redox process from the fast formation step. The absorption spectrophotometric data for $FeCbH_2^{2+}$ are given in Figure S6 in the Supporting Information and were processed[28−30] in order to determine the stability of this complex (Table 1).

Spectrophotometric titration of ferric chrysobactin complexes ($[Fe^{III}]_{tot}/[Cb]_{tot} = 1/4.2$) was performed between p[H] = 9.40 and 4.07 (Figure 3).

Above p[H] ~ 8.5, λ_{max} was constant at 493 nm, which is typical for the tris(catecholato)iron(III) complexes.[38] The visible spectra of the ferric chrysobactin system exhibited an isosbestic point at 550 nm in the p[H] range from 9.40 to 5.66, and λ_{max} of the charge-transfer (CT) absorption band underwent a bathochromic shift to 572 nm, which is characteristic of the bis(catecholato)iron(III) species.[38] Below p[H] = 5.66, a hypochromic shift with a slight concomitant bathochromic shift was observed. The spectral data recorded in the p[H] range between 9.40 and 5.66 were analyzed using the Specfit program.[28−30] Two absorbing species were determined, namely, $FeCb_2H_2^-$ and $FeCb_3H_3^{3-}$, and their respective global stability constants were thus calculated. These values are in very good agreement with those determined by potentiometry. The calculated electronic spectra of the ferric mono-, bis-, and tris(chrysobactin) complexes are given in Figure 4. The molar extinction coefficients corresponding to the maxima of the ligand-to-metal charge-transfer (LMCT) bands of $FeCbH_2^{2+}$, $FeCb_2H_2^-$, and $FeCb_3H_3^{3-}$ species are $\varepsilon_{680} = 1300$ M^{-1} cm^{-1}, $\varepsilon_{572} = 3700$ M^{-1} cm^{-1}, and $\varepsilon_{493} = 5300$ M^{-1} cm^{-1}, respectively, and are in excellent agreement with spectrophotometric data available in the literature for iron(III) bound to catechols.[4,19,47]

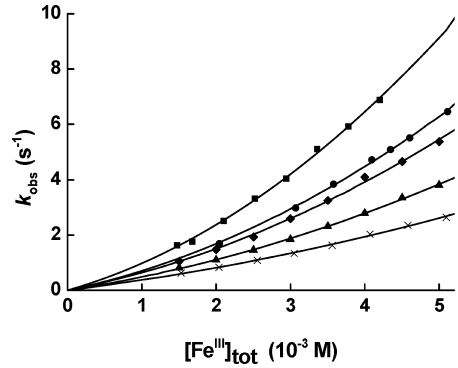

Figure 5. Variation of the pseudo-first-order rate constant k_{obs} relative to the formation of ferric mono(chrysobactin) as a function of $[Fe^{III}]_{tot}$ at different $[H^+]_{tot}$ (M): 0.0089 (■) 0.0112 (●), 0.0126 (◆), 0.0158 (▲), 0.0200 (×). Solvent = water; $I = 0.1$ M; $T = 25.0(2)$ °C.

Ferric Complex Formation Kinetics. A single-exponential signal versus time was recorded at 680 nm after mixing solutions of chrysobactin and iron(III) under acidic conditions (Figure S7 in the Supporting Information). The final absorbance was reached in less than 10 s, and no loss of spectrophotometric amplitude was observed during the dead time of the stopped-flow device (~3 ms). The variations of the corresponding pseudo-first-order rate constants (k_{obs}) with $[H^+]_{tot}$ and $[Fe^{III}]_{tot}$ are given in Figure 5 (Table S1 in the Supporting Information).

At a given $[H^+]_{tot}$, the variation of k_{obs} (s^{-1}) with $[Fe^{III}]_{tot}$ obeyed the following relationship:

$$k_{obs} = k_a[Fe^{III}]_{tot} + k_b[Fe^{III}]_{tot}^2 \quad (1)$$

The dependence of the rate constants k_a (M^{-1} s^{-1}) and k_b (M^{-2} s^{-1}) on the H^+ concentration is shown in Figure 6.

The formation mechanism of ferric chrysobactin $FeCbH_2^{2+}$ [reactions (5)−(9)] from two protonated forms of free chrysobactin, CbH_3 and CbH_4^+ [equilibrium (4)], with three iron(III) species, Fe^{3+}, $Fe(OH)^{2+}$, and $Fe_2(OH)_2^{2+}$ [equilibria (2) and (3)], satisfactorily accounts for our data. The protolytic (K_H) and dimerization (K_D) equilibria for the iron(III) species[48] can be considered as fast steps.[49] Therefore, the corresponding thermodynamic constants can be used in the kinetic equations. The same argument holds for equilibrium (4), which refers to the deprotonation of the carboxylic group of chrysobactin ($K_a = 1/K^H_4$). For the sake of simplicity, most of water molecules solvating the various iron(III) species have been omitted in our notations.

(47) (a) Jewett, S. L.; Eggling, S.; Geller, L. J. *Inorg. Biochem.* **1997**, *66*, 165–173. (b) Karpishin, T. B.; Gebhard, M. S.; Solomon, E. I.; Raymond, K. N. *J. Am. Chem. Soc.* **1991**, *113*, 2977–2984. (c) Dei, A. *Inorg. Chem.* **1993**, *32*, 5730–5733.
(48) Milburn, R. M.; Vosburgh, W. C. *J. Am. Chem. Soc.* **1955**, *77*, 1352–1355.
(49) Birus, M.; Kujundzic, N.; Pribanic, M. *Prog. React. Kinet.* **1993**, *18*, 171–271.

$$Fe(H_2O)_6^{3+} \underset{\text{fast}}{\overset{K_H}{\rightleftharpoons}} Fe(H_2O)_5(OH)^{2+} + H^+ \quad (2)$$

$$2Fe(H_2O)_6^{3+} \underset{\text{fast}}{\overset{K_D}{\rightleftharpoons}} Fe_2(H_2O)_{10}(OH)_2^{4+} + 2H^+ \quad (3)$$

$$CbH_4^+ \underset{\text{fast}}{\overset{K_a}{\rightleftharpoons}} CbH_3 + H^+ \quad (4)$$

$$Fe^{3+} + CbH_3 \xrightarrow{k_1} FeCbH_2^{2+} + H^+ \quad (5)$$

$$Fe(OH)^{2+} + CbH_4^+ \xrightarrow{k_2} FeCbH_2^{2+} + H^+ + H_2O \quad (6)$$

$$Fe(OH)^{2+} + CbH_3 \xrightarrow{k_3} FeCbH_2^{2+} + H_2O \quad (7)$$

$$Fe_2(OH)_2^{4+} + CbH_4^+ \xrightarrow{k_4} FeCbH_2^{2+} + Fe(OH)^{2+} + H^+ + H_2O \quad (8)$$

$$Fe_2(OH)_2^{4+} + CbH_3 \xrightarrow{k_5} FeCbH_2^{2+} + Fe(OH)^{2+} + H_2O \quad (9)$$

This mechanism leads to the following rate equation:

$$v = -\frac{d[Cb]}{dt} = k_{obs}([CbH_4^+] + [CbH_3]) \quad (10)$$

where [Cb] denotes the total concentration of the free ligand. At equilibrium and under our experimental conditions ($1.70 \leq p[H] \leq 2.05$), the concentrations of the $Fe(OH)_2^+$ and $Fe_2(OH)_2^{4+}$ species could be neglected and the total iron(III) concentration written as

$$[Fe^{III}]_{tot} = [Fe^{3+}] + [FeOH^{2+}] \quad (11)$$

Taking into account eqs 1, 10, and 11, equilibria (2)−(4), and reactions (5)−(9), the pseudo-first-order rate constant k_{obs} can be expressed as

$$k_{obs} = \frac{(k_1K_a + k_2K_H)[H^+]_{tot} + k_3K_HK_a}{([H^+]_{tot} + K_H)([H^+]_{tot} + K_a)}[Fe^{III}]_{tot} + \frac{k_4K_D[H^+]_{tot} + k_5K_aK_D}{([H^+]_{tot} + K_H)^2([H^+]_{tot} + K_a)}[Fe^{III}]_{tot}^2 \quad (12)$$

The rate constants k_a (M^{-1} s^{-1}) and k_b (M^{-2} s^{-1}) in eq 1 are now defined by eq 12. A nonlinear least-squares fitting of the variations of k_a and k_b versus $[H^+]_{tot}$ (Figure 6) allowed us to determine the rate constants included in reactions (5)−(9) [values of $K_H = 2.89 \times 10^{-3}$ M and $K_D = 1.42 \times 10^{-3}$ M were taken from ref 48, while K_a ($=1/K^4_H$) was determined in the present work (Table 1)]. The rate constants are calculated as $k_1K_a + k_2K_H = 6.1(5)$ s^{-1}, $k_3 = 1.6(3) \times 10^4$ M^{-1} s^{-1}, $k_4 = 1.2(1) \times 10^4$ M^{-1} s^{-1}, and $k_5 = 1.4(2) \times 10^5$ M^{-1} s^{-1}. Because of the well-known proton ambiguity,[49] it was not possible to separate the contributions of k_1 and k_2 in the rate law. However, taking into account that the reactivity of Fe^{3+} is generally 10^3 times lower than that of $Fe(OH)^{2+}$ species,[50,51] we can neglect the first term of the expression $k_1K_a + k_2K_H$ and the rate constant k_2 can be estimated as $k_2 = 2.1(2) \times 10^3$ M^{-1} s^{-1}. This value agrees well with those determined for the reaction of $Fe(OH)^{2+}$ species with catechol-type ligands.[49]

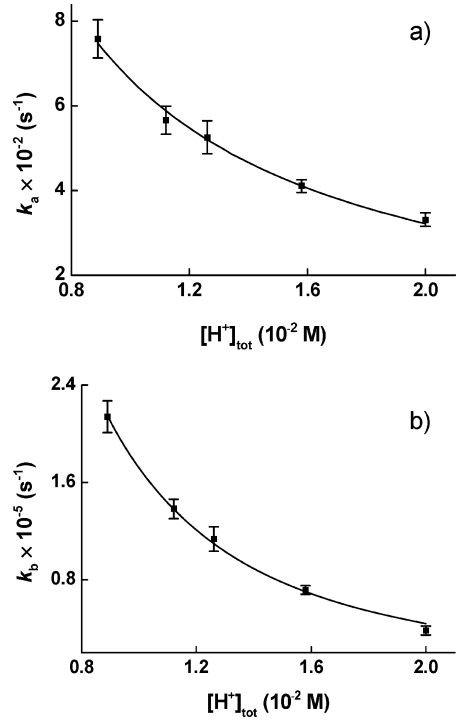

Figure 6. Dependence of the ferric mono(chrysobactin) complex formation rate coefficients k_a and k_b (eq 1) on $[H^+]_{tot}$. Lines represent the calculated fits using eq 12. Solvent = water; $I = 0.1$ M; $T = 25.0(2)$ °C.

Iron(III) Release Kinetics. In order to monitor the successive dissociation of each molecule of chrysobactin, the proton-promoted dissociations of ferric tris-, bis-, and mono(chrysobactin) complexes were studied separately under acidity conditions such that only one molecule of chrysobactin was released during each stage.

The dissociation of the ferric tris(chrysobactin) complex was carried out under such conditions that the main product formed was ferric bis(chrysobactin) species $FeCb_2H_2^-$. The decrease of absorbance at 493 nm was exponential in time, and the absorbance extrapolated to zero time corresponded to that of the ferric tris(chrysobactin) complex (Figure S8 in the Supporting Information). It is noteworthy that the absorption spectrum of the final product was in excellent agreement with that of ferric bis(chrysobactin) complex (Figure S8 in the Supporting Information). The global reaction can thus be written as

$$FeCb_3H_3^{3-} + 2H^+ \rightarrow FeCb_2H_2^- + CbH_3 \quad (13)$$

The pseudo-first-order rate constant k_{obs1} linearly varies with the $[H^+]_{tot}$ concentration (Figure 7a) in the entire p[H] range investigated, and the ordinate at the origin was not significant.

(50) Eigen, M.; Wilkins, R. G. *Adv. Chem. Ser.* **1965**, *49*, 55–67.
(51) (a) Grant, M.; Jordan, R. B. *Inorg. Chem.* **1981**, *20*, 55–60. (b) Helm, L.; Merbach, A. E. *Chem. Rev.* **2005**, *105*, 1923–1959. (c) Richens, D. T. *Chem. Rev.* **2005**, *105*, 1961–2002.

$$k_{obs1} = k_6[H^+]_{tot} \quad (14)$$

The bimolecular rate constant k_6 was calculated to be $1.13(1) \times 10^7\ M^{-1}\ s^{-1}$. The linear dependence of k_{obs1} with $[H^+]_{tot}$ suggests that the dissociation of the first chrysobactin ligand from $FeCb_3H_3^{3-}$results from the attack of one proton [reaction (15)]. The second proton involved in the global reaction (13) is related to the fast protonation of CbH_2^- species [equilibrium (16)].

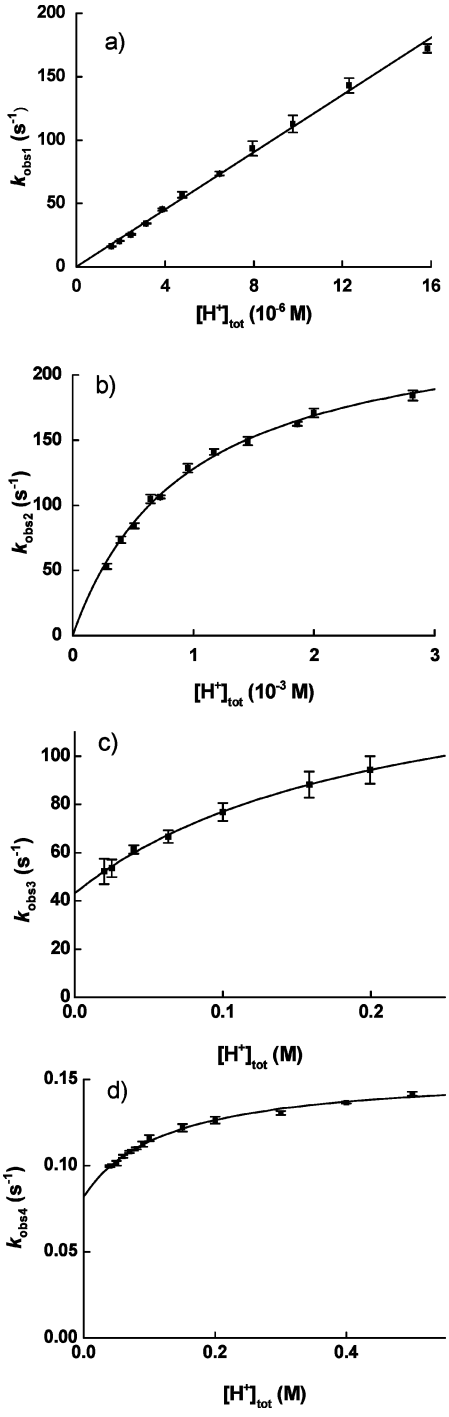

Figure 7. Variations of the pseudo-first-order rate constants for the dissociation of ferric chrysobactin complexes with $[H^+]_{tot}$. Solvent = water; $I = 1.0$ M ($NaClO_4$); $T = 25.0(2)$ °C. Error bars correspond to the standard deviation. The solid lines are the calculated fits. (a) Conversion of the tris complex to the bis complex. $[Cb]_{tot} = 3.0 \times 10^{-4}$ M; $[Fe^{III}]_{tot} = 7.45 \times 10^{-4}$ M. (b) Conversion of the bis complex to the mono complex. $[Cb]_{tot} = 2.1 \times 10^{-4}$ M; $[Fe^{III}]_{tot} = 1.02 \times 10^{-4}$ M. (c) Dissociation of the mono complex, first step. $[Cb]_{tot} = 2.4 \times 10^{-4}$ M; $[Fe^{III}]_{tot} = 1.16 \times 10^{-4}$ M. (d) Dissociation of the mono complex, second step. $[Cb]_{tot} = 3.2 \times 10^{-4}$ M; $[Fe^{III}]_{tot} = 1.59 \times 10^{-4}$ M.

$$FeCb_3H_3^{3-} + H^+ \xrightarrow{k_6} FeCb_2H_2^- + CbH_2^- \quad (15)$$

$$CbH_2^- + H^+ \underset{\text{fast}}{\overset{K_3^H}{\rightleftharpoons}} CbH_3 \quad (16)$$

The acid-triggered dissociation of the ferric bis(chrysobactin) complex led to the ferric mono(chrysobactin) species $FeCbH_2^{2+}$, as evidenced by the absorption spectrum recorded at the end of the reaction [reaction (17)]. The absorbance at 572 nm was monitored and decreased exponentially versus time (Figure S9 in the Supporting Information). Moreover, a significant loss of the spectrophotometric signal amplitude (~40%) during the mixing time of the fast-mixing device was observed. The global reaction can be written as

$$FeCb_2H_2^- + 3H^+ \rightarrow FeCbH_2^{2+} + CbH_3 \quad (17)$$

The variation of the pseudo-first-order rate constant k_{obs2} with $[H^+]_{tot}$ is shown in Figure 7b. The experimental kinetic data were processed using the following equation:

$$k_{obs2} = \frac{K_1 k_7 [H^+]_{tot}}{1 + K_1[H^+]_{tot}} \quad (18)$$

The constants K_1 and k_7 were found to be $1.06(6) \times 10^3\ M^{-1}$ and $248(6)\ s^{-1}$, respectively.[52] The following mechanism for the dissociation of the $FeCb_2H_2^-$ complex is proposed:

$$FeCb_2H_2^- + H^+ \underset{\text{fast}}{\overset{K_1}{\rightleftharpoons}} FeCb_2H_3^* \quad (19)$$

$$FeCb_2H_3^* \xrightarrow{k_7} FeCbH^+ + CbH_2^- \quad (20)$$

$$FeCbH^+ + H^+ \underset{\text{fast}}{\rightleftharpoons} FeCbH_2^{2+} \quad (21)$$

$$CbH_2^- + H^+ \underset{\text{fast}}{\overset{K_3^H}{\rightleftharpoons}} CbH_3 \quad (22)$$

A fast-protonation preequilibrium [K_1, equilibrium (19)] can account for the saturation behavior of k_{obs2} versus $[H^+]_{tot}$. The protonated ferric bis(chrysobactin) intermediate $FeCb_2H_3^*$ then undergoes a ligand release in the rate-determining step [reaction (20)]. Further protonations of ferric mono(chrysobactin) complex $FeCbH^+$ [equilibrium (21)] and free ligand CbH_2^- [equilibrium (22)] take place in fast equilibria.

The global reaction that describes the dissociation of the ferric mono(chrysobactin) complex can be expressed as follows:

(52) Scarrow, R. C.; Ecker, D. J.; Ng, C.; Liu, S.; Raymond, K. N. *Inorg. Chem.* **1991**, *30*, 900–906.

$$FeCbH_2^{2+} + 2H^+ \rightarrow Fe^{3+} + CbH_4^+ \quad (23)$$

The reaction proceeds in two well-separated stages, which are hereafter designed as the faster step and the slower one.

The faster step (Figure S10 in the Supporting Information) results as an exponential decrease of absorbance at 680 nm versus time and was completed in less than 100 ms. The variation of the pseudo-first-order rate constant k_{obs3} with $[H^+]_{tot}$ is given in Figure 7c. The experimental kinetic data could be fitted using the following equation:

$$k_{obs3} = \frac{K_2 k_8 [H^+]_{tot}}{1 + K_2 [H^+]_{tot}} + k_{-8} \quad (24)$$

with $K_2 = 5(1)\ M^{-1}$,[53] $k_8 = 105(10)\ s^{-1}$, and $k_{-8} = 43(2)\ s^{-1}$.

The slower step is characterized by a further decrease of absorbance at 680 nm with time and was completed in less than 100 s (Figure S11 in the Supporting Information). For $[H^+]_{tot} > 0.15$ M, the final absorbance at 680 nm is close to zero, while for lower $[H^+]_{tot}$, a residual absorbance at the end of the reaction is observed. The variation of the pseudo-first-order rate constant k_{obs4} with $[H^+]_{tot}$ is given in Figure 7d. The experimental data were fitted according to the following equation:

$$k_{obs4} = \frac{K_3 k_9 [H^+]_{tot}}{1 + K_3 [H^+]_{tot}} + k_{-9} \quad (25)$$

with $K_3 = 8(2)\ M^{-1}$, $k_9 = 7.2(2) \times 10^{-2}\ s^{-1}$, and $k_{-9} = 8.2(4) \times 10^{-2}\ s^{-1}$. For this two-step dissociation of the $FeCbH_2^{2+}$ complex, the following process can be suggested:

Faster step:

$$FeCbH_2^{2+} + H^+ \underset{fast}{\overset{K_2}{\rightleftharpoons}} FeCbH_3^{3+}* \quad (26)$$

$$FeCbH_3^{3+}* \underset{k_{-8}}{\overset{k_8}{\rightleftharpoons}} FeCbH_3^{3+}** \quad (27)$$

Slower step:

$$FeCbH_3^{3+}** \underset{k_{-9}}{\overset{k_9}{\rightleftharpoons}} Fe^{3+} + CbH_3 \quad (28)$$

$$CbH_3 + H^+ \underset{fast}{\overset{K_4^H}{\rightleftharpoons}} CbH_4^+ \quad (29)$$

Attack of a proton occurs during a fast-protonation preequilibrium [equilibrium (26)] and leads to an intermediate ferric species $FeCbH_3^{3+}*$, which is rearranged in the first rate-determining step [equilibrium (27)] into an intermediate $FeCbH_3^{3+}**$ complex. The second rate-limiting step [equilibrium (28)] is then related to the dissociation of the $FeCbH_3^{3+}**$ intermediate to lead to the ferric ion Fe^{3+} and to the ligand CbH_3. The released chrysobactin molecule experiences further fast protonation according to the acidity of the medium [equilibrium (29)]. Steps (26) and (27) can be considered as fast preequilibria with respect to step (28),

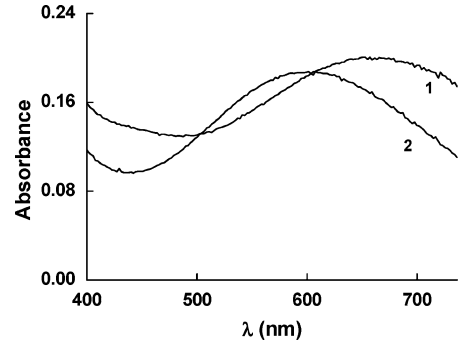

Figure 8. Absorption spectra recorded during the dissociation of the ferric mono(chrysobactin) complex using a diode-array detector. $[Cb]_{tot} = 2.4 \times 10^{-4}$ M; $[Fe^{III}]_{tot} = 1.16 \times 10^{-4}$ M; $l = 1$ cm; $t = 34.56$ ms; solvent = water; $I = 1.0$ M ($NaClO_4$); $T = 25.0(2)$ °C. $[H^+]_{tot} = 0.02$ M (**1** and 0.16 M (**2**).

as confirmed by the fair agreement between the value of K_3 (eq 25) and that of $K_2k_8/k_{-8} = 12(3)\ M^{-1}$ (eq 24).

In order to characterize the $FeCbH_3^{3+}**$ intermediate, kinetic measurements were carried out using a diode-array detector. Figure 8 shows the absorption spectra recorded at the end of the faster step for the dissociation of the ferric mono(chrysobactin) complex [step (27)] at two different $[H^+]_{tot}$.

The absorption spectrum measured at $[H^+]_{tot} = 0.02$ M possesses a maximum centered at ~660 nm, while that recorded at $[H^+]_{tot} = 0.16$ M is characterized by an absorption maximum at ~590 nm. The spectra presented in Figure 8 clearly show that $FeCbH_3^{3+}*$ is a mono(catecholate) complex with a LMCT band centered at ~700 nm,[54] while $FeCbH_3^{3+}**$ corresponds to a mono(salicylate) species with a LMCT band centered at ~590 nm.[55,56]

Discussion and Conclusion

Acido−Basic Properties of Chrysobactin. The protonation constants were attributed by comparison with analogous compounds (Figure 1). The second protonation constant, log $K_2^H = 10.61(1)$, agrees well with the reported values for the ϵ-amine of lysine[57] (log $K^H = 10.65$) and lysylglycine[58] (log $K^H = 10.72$) and was attributed to the ϵ-amine of the lysyl residue of chrysobactin. The third protonation constant, log $K_3^H = 6.73(1)$, was assigned to the *o*-hydroxyl proton. The lower basicity of the *o*-hydroxyl group of chrysobactin compared to catechol[59] (log $K_2^H = 9.13$) is due to the electron-withdrawing effect of the amide moiety and the stabilization of the deprotonated *o*-hydroxyl through an intramolecular hydrogen bond in a six-membered ring with the amide hydrogen (Figure 1). These two effects are well documented in the literature for 2,3-dihydroxybenzoyl

(53) Jordan, R. B. *Inorg. Chem.* **1983**, *22*, 4160–4161.
(54) Avdeef, A.; Sofen, S. R.; Bregante, T. L.; Raymond, K. N. *J. Am. Chem. Soc.* **1978**, *100*, 5362–5370.
(55) Ogawa, K.; Tobe, N. *Bull. Chem. Soc. Jpn.* **1966**, *39*, 227–232.
(56) Albrecht-Gary, A. M.; Blanc, S.; Biaso, F.; Thomas, F.; Baret, P.; Gellon, G.; Pierre, J. L.; Serratrice, G. *Eur. J. Inorg. Chem.* **2003**, 2596–2605.
(57) Lekchiri, A.; Morcellet, M.; Wozniak, M. *Polyhedron* **1987**, *6*, 633–639.
(58) Sayer, T.; Rabenstein, D. *Can. J. Chem.* **1976**, *54*, 3392–3400.
(59) Zhu, D.-H.; Kappel, M. J.; Raymond, K. N. *Inorg. Chim. Acta* **1988**, *147*, 115–121.

derivatives such as *N*-(2,3-dihydroxybenzoyl)dipeptides,[60] *N*-ethyl-2,3-dihydroxybenzamide,[5] *N*-methyl-2,3-dihydroxybenzamide[61] or synthetic analogues of enterobactin.[62] Depending on the state of protonation of the *o*-phenol/phenolate group, an intramolecular hydrogen bond with either the C=O or N−H function of the amide group takes place thanks to a rotation of 180° around the amide bond (Figure S13 in the Supporting Information). This structural feature confers to catechol amide ligands analogous to enterobactin peculiar acidio−basic properties ($7.0 < \log K^{H} < 7.4$).[59−61] Nevertheless, this is still slightly higher than log K_3^{H} of chrysobactin. A plausible explanation can be that this protonation constant is further lowered because of intramolecular interactions between the carbonyl amide group and the residues from the peptidic chain of chrysobactin, as suggested in Figure S13 in the Supporting Information. It can be also seen that the lysine residue is bent toward the carboxylate of the serine residue and its ϵ-ammonium group interacts with the carboxylate oxygens via multiple hydrogen bonds and electrostatic interactions.

The last protonation constant of chrysobactin, log K_4^{H} = 3.17(1), was attributed to the serine terminal carboxylate group. The value is in agreement with the protonation constant of the terminal carboxylate in glycylserine[63] (log K^{H} = 2.99). The protonation constants of chrysobactin, which were herein determined, confirm the qualitative observations, published by Persmark et al.[7] These authors indeed found that chrysobactin had a net charge 1+ at p[H] = 1.9 and was neutral at p[H] = 4.4 and 6.5. According to the distribution diagrams (Figure S5 in the Supporting Information), at p[H] = 1.9, chrysobactin is mainly present in the form of CbH_4^{+} species, while, at p[H] ∼ 5, the only protonated form of chrysobactin is the neutral CbH_3 species.

Stability Constants of Ferric Chrysobactin Complexes. Until now, the only stability constant for ferric chrysobactin complexes was published by Persmark and Neilands.[19] The "cumulative equilibrium constant β_3", defined as $[Fe(HCb)_3^{3-}]/[Fe^{3+}][HCb^{2-}]^3$, was determined by potentiometry (log β_3 = 35.4). Assuming that in $FeCb_3H_3^{3-}$ three protons are bound to the ϵ-amines of chrysobactins and that the protonations do not affect the complexation of iron(III), log β_3 is equal to log $\beta_{FeCb_3H_3} - 3 \times \log K_1^{H}$ = 35.8, in agreement with the value previously published.[19] Furthermore, the values of λ_{max} and the corresponding molar absorption coefficients for bis- and tris(chrysobactin)iron(III) complexes determined in our work (Figure 4) are in good agreement with those determined by Persmark and Neilands.[19] Using the protonation and stability constants given in Table 1, distribution diagrams were calculated for $[Fe^{III}]_{tot} = 10^{-3}$ M and $[Cb]_{tot} = 4 \times 10^{-3}$ M (Figure S12 in the Supporting Information) and for $[Fe^{III}]_{tot} = 10^{-6}$ M and $[Cb]_{tot} = 4 \times 10^{-5}$ M, which are relevant conditions for phytobacteria (Figure 9).

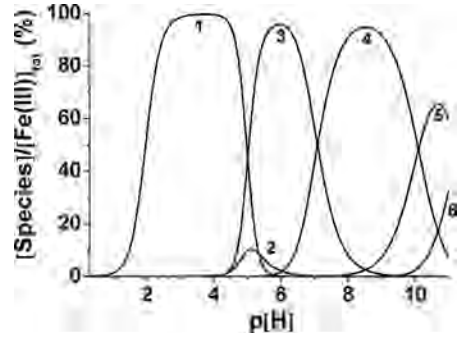

Figure 9. Distribution diagram of ferric chrysobactin complexes. $[Fe^{III}]_{tot} = 1.0 \times 10^{-6}$ M; $[Cb]_{tot} = 4 \times 10^{-5}$ M; solvent = water; I = 0.1 M ($NaClO_4$); T = 25.0 °C. (**1**) $FeCbH_2^{2+}$; (**2**) $FeCb_2H_3$ (**3**) $FeCb_2H_2^{-}$; (**4**) $FeCb_3H_3^{3-}$; (**5**) $FeCb_3H_2^{4}$; (**6**) $FeCb_3H^{5-}$.

Interestingly, it shows that, at p[H] = 6.5, a mixture of ferric bis- and tris(chrysobactin) complexes is present, in agreement with qualitative observations.[19] We calculated the structures of $GaCb_3H_3^{3-}$ and $GaCb_2H_2^{-}$ complexes (Figure 10). Intramolecular hydrogen bonds are formed between the *o*-phenolate oxygens and the neighboring γ-N−H groups (Figure 10), in agreement with X-ray structures available for analogous 2,3-dihydroxybenzamide-type chelators.[64,65] Moreover, electrostatic interactions could take place between the dipeptidic parts of two neighboring chrysobactins, leading to an organized peptidic system resembling the cyclic triester scaffold of enterobactin (Figure 10).

In order to compare the iron(III) coordination properties of chrysobactin with those of other natural iron(III) chelators, the corresponding pFe values,[66] which measure the equilibrium concentrations of free iron(III), are listed in Table 2. These pFe values were calculated at p[H] = 6.5, which corresponds to the acidity in plants apoplasm.[12,67,68] For the sake of comparison, pFe values calculated at pH = 7.4 are also given. Obviously, chrysobactin is a weaker iron(III) binder than hexadentate siderophores, such as enterobactin[39] or ferrioxamine B.[69] However, chrysobactin exhibits higher pFe values than citrate or malate, which are known to be

(60) Kozlowski, H.; Radomska, B.; Kiss, T.; Balla, J.; Nakonieczna, L.; Pastuszak, J. J.; Langelier, Y. *J. Inorg. Biochem.* **1991**, *43*, 779–787.
(61) Escalada, J.; Freedman, D.; Werner, E. J. *Acta Crystallogr.* **2004**, *E60*, o1296–o1298.
(62) Hou, Z.; Stack, T. D. P.; Sunderland, C. J.; Raymond, K. N. *Inorg. Chem. Acta* **1997**, *263*, 341–355.
(63) Maslowska, J.; Chruscinski, L. *Polyhedron* **1986**, *5*, 1135–1139.
(64) (a) McMurry, T. J.; Hosseini, M. W.; Garrett, T. M.; Hahn, F. E.; Reyes, Z. E.; Raymond, K. N. *J. Am. Chem. Soc.* **1987**, *109*, 7196–7198. (b) Garrett, T. M.; McMurry, T. J.; Hosseini, M. W.; Reyes, Z. E.; Hahn, F. E.; Raymond, K. N. *J. Am. Chem. Soc.* **1991**, *113*, 2965–2977. (c) Stack, T. D. P.; Karpishin, T. B.; Raymond, K. N. *J. Am. Chem. Soc.* **1992**, *114*, 1512–1514. (d) Karpishin, T. B.; Stack, T. D. P.; Raymond, K. N. *J. Am. Chem. Soc.* **1993**, *115*, 182–192. (e) Karpishin, T. B.; Stack, T. D. P.; Raymond, K. N. *J. Am. Chem. Soc.* **1993**, *115*, 6115–6125.
(65) Dertz, E. A.; Xu, J.; Raymond, K. N. *Inorg. Chem.* **2006**, *45*, 5465–5478.
(66) Harris, W. R.; Carrano, C. J.; Raymond, K. N. *J. Am. Chem. Soc.* **1979**, *101*, 2213–2214.
(67) Nachin, L.; Barras, F. *Mol. Plant−Microbe Interact.* **2000**, *13*, 882–886.
(68) Grignon, C.; Sentenac, H. *Annu. Rev. Plant Physiol.* **1991**, *42*, 103–128.
(69) (a) Evers, A.; Hancock, R. D.; Martell, A. E.; Motekaitis, R. J. *Inorg. Chem.* **1989**, *28*, 2189–2195. (b) Kornreich-Leshem, H.; Ziv, C.; Gumienna-Kontecka, E.; Arad-Yellin, R.; Chen, Y.; Elhabiri, M.; Albrecht-Gary, A. M.; Hadar, Y.; Shanzer, A. *J. Am. Chem. Soc.* **2005**, *127*, 1137–1145.

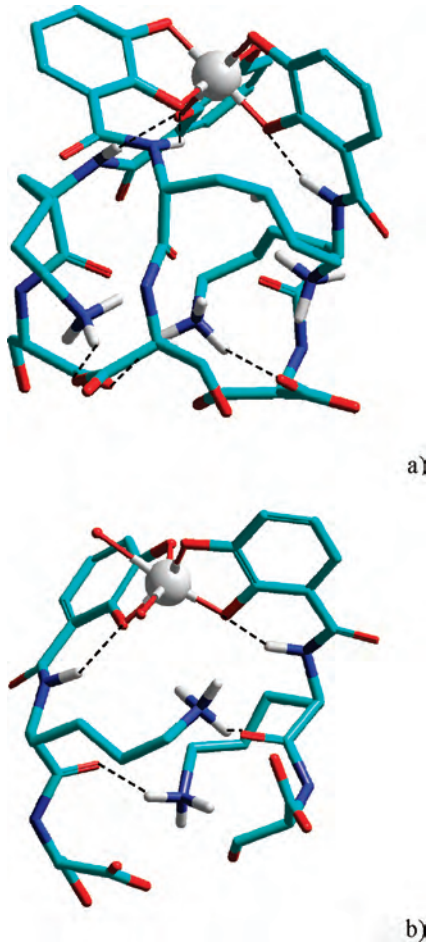

Figure 10. Calculated structures of gallium(III) chrysobactin complexes (a) *fac*-(Λ)$GaCb_3H_3^{3-}$ and (b) (Λ)$GaCb_2H_2^{-}$ (molecular modeling performed with the Hyperchem 7.5 program at the PM3 level). The interstrand and intrastrand hydrogen bonds are included as dotted lines (distances ranging from 1.7 to 2 Å).

Table 2. Comparison of the Free Iron(III) Concentrations Expressed as pFe = −log $[Fe^{III}]$[a]

ligand L	pFe pH = 6.5	pFe pH = 7.4
enterobactin[39]	29.8	35.5
ferrioxamine B[69]	24.2	26.9
o,*o*-EDDHA[b,14]	24.0	26.9
chrysobactin	14.6	17.3
DMB[c,38,66]	12.5	∼15
citric acid[70,71]	11.8	11.8
malic acid[71]	11.2	12.3

[a] $[L]_{tot} = 10^{-5}$ M, $[Fe^{III}]_{tot} = 10^{-6}$ M. [b] Ethylenediamine-*N*,*N*′-bis(2-hydroxyphenylacetic acid). [c] 2,3-Dihydroxy-*N*,*N*-dimethylbenzamide.

the major plant iron ligands,[13] and can effectively sequester iron(III) from their ferric complexes.

Formation Kinetics. We have summarized in Table 3 the rate constants relative to the reaction of $Fe(OH)^{2+}$ with various chelators. Inspection of Table 3 clearly indicates that, either with neutral or with negatively charged binding sites, the reactivity of $Fe(OH)^{2+}$ is independent of the chemical structure of the ligands. However, the charge of the coordination moiety strongly influences the binding rate constants because they are varying about 1 order of magnitude (Table 3). These results suggest a I_d dissociative Eigen−Wilkins mechanism[72] with a fast outer-sphere complex preequilibrium (K_{os}), followed by a rate-limiting step involving the desolvation of the metal ion (k_{ex}).

Table 3. Comparison of the Reactivity of $Fe(OH)^{2+}$ with Chrysobactin and Various Chelators

compound	neutral reaction site k_f (10^3 M^{-1} s^{-1})	negatively charged reaction site k_f ($10^4 M^{-1}$ s^{-1})	ref
chrysobactin[a]	2.1(2)	1.6(3)[e]	this work
pyoverdin PaA[b]	7.7(4)		83
azotobactin τ[b]	5.9(4)	2.1(3)	73
ferrioxamine B[b]	3.6(2)		74 and 75
acetohydroxamic acid[c]	5.65(0.864)		79
catechol	3.1(2)		76
tiron[c]	3.08(0.48)		80
salicylic acid	3.5	1.5	80
2,3-dihydroxybenzoic acid[c]	4.8	<3	80
phenol	1.5		80
tartaric acid	5.1	2.2	77
citric acid	3.1	2.6	77
phosphate[d]		0.47(1)	78

[a] Solvent = water, $T = 25$ °C, $I = 0.1$ M ($NaClO_4$). [b] Solvent = water, $T = 25$ °C, $I = 2.0$ M ($NaClO_4$). [c] Solvent = water, $T = 25$ °C, $I = 1.0$ M ($NaClO_4$). [d] Solvent = water, $T = 10$ °C, $I = 1$ M ($NaClO_4$). [e] The serine carboxylic group is assumed to be the initial reaction site (see the text).

$$k_{Fe(OH)^{2+}} = K_{os}k_{ex} \quad (30)$$

The values of the formation rate constants, k_f, determined for the two protonated forms of chrysobactin, CbH_4^+ and CbH_3, agree well with those of the other ligands having a neutral or negatively charged reaction center, respectively (Table 3). Considering that in CbH_4^+ the serine carboxylic group is protonated (Figure 1) and that in CbH_3 this unit is deprotonated, our data could indicate that the initial binding site of $Fe(OH)^{2+}$ would be the terminal carboxylate. NMR studies of gallium(III) complexes of chrysobactin[19] evidenced that the carboxylic group was not involved in the final coordination of the cation. That was also emphasized in the present work by measuring the LMCT absorption bands typical for the ferric catecholate complexes. It can thus be envisaged that the ferric ion, initially bound to the carboxylate group, rapidly translocates to the catecholate moiety of chrysobactin. The complexation rate of $Fe(OH)^{2+}$ with chrysobactin is tuned by the protonation state of its carboxylic function during the formation of the corresponding outer-sphere complex ($K_{os} = 13.3 \times 10^{-2}$ M^{-1} for CbH_3, $K_{os} = 1.75 \times 10^{-2}$ M^{-1} for CbH_4^+).[51]

(70) (a) Ramamoorthy, S.; Manning, P. *J. Inorg. Nucl. Chem.* **1973**, *35*, 1571–1575. (b) Warner, R. C.; Weber, I. *J. Am. Chem. Soc.* **1953**, *75*, 5086–5094.
(71) Timberlake, C. *J. Chem. Soc.* **1964**, 5078–5085.
(72) (a) Eigen, M.; Wilkins, R. G. *Adv. Chem. Ser.* **1965**, *49*, 55–67. (b) Eigen, M. *Z. Electrochem.* **1960**, *64*, 115–123.
(73) (a) Palanché, T. Méchanismes de coordination du fer: Applications biologiques et analytiques. Ph.D. Thesis, Université Louis Pasteur, Strasbourg, France, 1995. (b) Palanché, T.; Blanc, S.; Hennard, C.; Abdallah, M. A.; Albrecht-Gary, A. M. *Inorg. Chem.* **2004**, *43*, 1137–1152.
(74) Birus, M.; Bradic, Z.; Krznaric, G.; Kujundzic, N.; Pribanic, M.; Wilkins, P. C.; Wilkins, R. G. *Inorg. Chem.* **1987**, *26*, 1000–1005.
(75) Batinic-Haberle, I.; Birus, M.; Pribanic, M. *Inorg. Chem.* **1991**, *30*, 4882–4887.
(76) Mentasti, E.; Pelizzetti, E. *J. Chem. Soc., Dalton Trans.* **1973**, 2605–2608.
(77) Mentasti, E.; Baiocchi, C. *J. Coord. Chem.* **1980**, *10*, 229–237.
(78) Lente, G.; Magalhaes, M. E. A.; Fabian, I. *Inorg. Chem.* **2000**, *39*, 1950–1954.

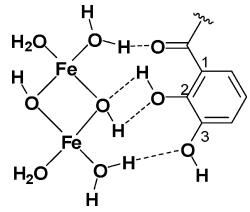

Figure 11. Precursor complex of chrysobactin with $Fe_2(OH)_2^{4+}$.

Table 4. Comparison of the Reactivity of $Fe_2(OH)_2^{4+}$ with Chrysobactin and Various Compounds

compound	neutral reaction site k_f (10^4 M^{-1} s^{-1})	negatively charged reaction site k_f (10^5 M^{-1} s^{-1})	ref
chrysobactin[a]	1.2(1)	1.4(2)	this work
pyoverdin PaA[b]		0.50(6)	83
azotobactin τ[b]		6.1(3)	73
acetohydroxamic acid[c]		0.85(0.135)	79
tiron[c]	1.09(3)		80
2,3-dihydroxybenzoic acid[c]	0.45(0.55)	2.15(0.88)	80

[a] Solvent = water, T = 25 °C, I = 0.1 M ($NaClO_4$). [b] Solvent = water, T = 25 °C, I = 2.0 M ($NaClO_4$). [c] Solvent = water, T = 25 °C, I = 1.0 M ($NaClO_4$).

The nonlinear relationship between the pseudo-first-order rate constant k_{obs} and the total iron(III) concentration can be explained by the reactivity of the ferric dimeric species $Fe_2(OH)_2^{4+}$.[49,79−83] The rate-limiting step is related to the formation of a precursor complex involving interactions of the 1-carboxamide substituent and of the 3-hydroxyl of the catechol ring with both iron(III) centers of the dimeric reactant (Figure 11). The dimeric complex dissociates rapidly, giving FeL.

The corresponding kinetic parameters (Table 4) evidence the higher reactivity of $Fe_2(OH)_2^{4+}$ with CbH_3 and CbH_4^+, when compared with $Fe(OH)^{2+}$ (Table 3).[4] Furthermore, the significantly higher reactivity of CbH_3 compared to CbH_4^+ (k_5/k_4 = 11.7) again suggests the participation of the carboxylate group in the iron(III) chelation mechanism (Table 4).

Dissociation Kinetics. Although the proton-promoted dissociation of ferric siderophore complexes is accepted as one of the possible mechanisms of intracellular iron release in bacteria, the literature dealing with the kinetics of acid dissociation of ferric catecholate complexes is rather scarce. Except the thorough kinetic study of acid dissociation of ferric complexes of tiron published by Zhang and Jordan[84] and our ongoing kinetics investigations on dietary iron(III) chelators (β-glucogallin, catechin and quercetin),[85] no other systematic survey on this subject is known to the authors.

(79) (a) Birus, M.; Kujundzic, N.; Pribanic, M. *Inorg. Chim. Acta* **1980**, *55*, 65–69. (b) Jordan, R. B.; Xu, J. H. *Pure Appl. Chem.* **1988**, *60*, 1205–1208.
(80) Xu, J.; Jordan, R. B. *Inorg. Chem.* **1988**, *27*, 1502–1507.
(81) Serratrice, G.; Zeghli, A.; Béguin, C. G.; Baret, P.; Pierre, J. L. *New J. Chem.* **1993**, *17*, 297–307.
(82) Serratrice, G.; Mourral, C.; Zeghli, A.; Béguin, C. G.; Baret, P.; Pierre, J. L. *New J. Chem.* **1994**, *17*, 749–758.
(83) Albrecht-Gary, A. M.; Blanc, S.; Rochel, N.; Ocaktan, A. Z.; Abdallah, M. A. *Inorg. Chem.* **1994**, *33*, 6391–6402.
(84) Zhang, Z.; Jordan, R. B. *Inorg. Chem.* **1996**, *35*, 1571–1576.
(85) (a) Marmolle, F. Propriétés de coordination métallique de polyphénols. Ph.D. Thesis, Université Louis Pasteur, Strasbourg, France, 1999. (b) Marcoux, S. Biodisponibilité de cations divalents et trivalents: propriétés et mécanismes de coordination de polyphénols du régime alimentaire. Ph.D. Thesis, Université Louis Pasteur, Strasbourg, France, 2001.

Table 5. Comparison of the Rate Constants for Dissociation of Chrysobactin and Tiron Iron(III) Complexes[a]

chrysobactin	tiron[84]
$k_6 = 1.13(1) \times 10^7$ M^{-1} s^{-1}	$k_{-3} = 1.7 \times 10^7$ M^{-1} s^{-1}
$K_1k_7 = 2.6 \times 10^5$ M^{-1} s^{-1}	$k_{-2} > 2.8 \times 10^5$ M^{-1} s^{-1}
$K_2(k_8/k_{-8})k_9 \sim 0.7$ M^{-1} s^{-1}	$k_{-1} = 1.2$ M^{-1} s^{-1}

[a] Solvent = water, T = 25 °C, I = 1.0 ($NaClO_4$).

Scheme 1

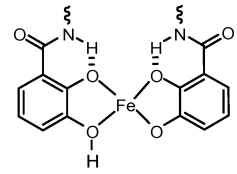

$FeCb_2H_3$*

Scheme 2

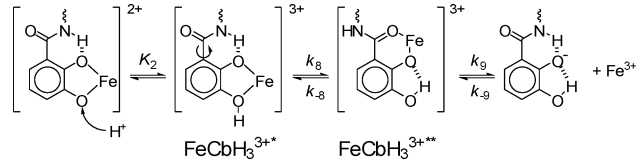

$FeCbH_3^{3+*}$ $FeCbH_3^{3+**}$

The proton-driven dissociation of the ferric tris(chrysobactin) complex proceeds via four steps involving three protonations (Figure 7). Taking tiron as a model,[84] we compare in Table 5 the bimolecular step-by-step release of chrysobactin from its ferric tris(chelate) complex under acidic conditions, according to the following equation:

$$FeL_nH + H \xrightarrow{k_{-n}} FeL_{n-1} + LH_2 \qquad (31)$$

where n = 1−3 and FeL_nH stands for a ferric protonated complex on one phenolic oxygen of the ligand to be released (charges omitted for the sake of simplicity). Furthermore, it was found that the dissociation of the ferric mono(tiron) complex also proceeds via the following pathway:

$$FeLH \xrightarrow{k_{-n}'} Fe(OH) + LH_2 \qquad (32)$$

A decrease of 2 orders of magnitude in the corresponding rate constants characterizes the loss of the first ligand compared to the second one, while a decrease of about 5 orders of magnitude corresponds to the dissociation of the third catechol around iron(III) for chrysobactin and tiron (Table 5). Electrostatic repulsions between the phenolate oxygens of the chrysobactin molecules in the tris and bis complexes accelerate the ligand release.

The stabilization of kinetic intermediates in the case of chrysobactin could be explained by hydrogen bonding between the catechol and the amide groups as illustrated below for the ferric bis(chelate) chrysobactin $FeCb_2H_3$* (eq 19).[86]

The release of the last chrysobactin molecule from $FeCbH_2^{2+}$ goes via two kinetic intermediates, $FeCbH_3^{3+*}$ and

(86) Diebler, H.; Secco, F.; Venturini, M. *J. Phys. Chem.* **1987**, *91*, 5106–5111.

$FeCbH_3^{3+**}$, which could correspond to catecholate and salicylate binding modes, with $\lambda^{max} = 700$ and 590 nm, respectively.

It now becomes clear why the mechanism of the dissociation of the first two chrysobactin ligands is different from that of the last one. The formation of an intermediate with the salicylate-type mode[87] of bonding requires the rotation of the catechoyl moiety around the $C_{amide}-C_{ar}$ bond, which is impossible because of steric hindrance of the dipeptidic residue of chrysobactin in tris- and bis(chrysobactin) complexes. Interestingly, these dissociation kinetic data support the fact that intracellular iron removal from chrysobactin in vivo does not require enzymatic degradation of this ligand.

Conclusion

We have presented an extensive physicochemical study of the binding properties of iron(III) by chrysobactin, a monocatecholate-type siderophore produced by the phytopathogenic bacterium *E. chrysanthemi*. The intricate biological role of chrysobactin in the virulence of *E. chrysanthemi* requires a better understanding of its physicochemical properties. We have therefore determined the protonation constants of the free ligand, characterized the various ferric species of chrysobactin, and determined the corresponding stability constants. The knowledge of these thermodynamic parameters allowed us to model the iron(III) uptake by chrysobactin under conditions (p[H] = 6.5, $[Fe]_{tot} = 10^{-6}$ M, $[Cb]_{tot} = 4 \times 10^{-5}$ M) that are relevant for phytobacteria (Figure 9). Ferric bis(chrysobactin) complex $FeCb_2H_2^-$ is clearly the predominant species and was found to be formed in combination with a small amount of the tris(chelate) $FeCb_3H_3^{3-}$.

Combining the physicochemical and biological data helped to address questions in relation to the recognition process of chrysobactin by its outer-membrane receptor Fct.[15] We showed that the calculated structure of the tris(chelate) gallium(III) complex resembles the one of ferric enterobactin due to the formation of an organized peptidic scaffold, which mimics the cyclic triester anchor of enterobactin. Despite this likeness, enterobactin is by far a stronger chelator than chrysobactin, as shown by the significantly different pFe values ($pFe^{ent} = 29.8$ and $pFe^{Cb} = 14.5$ at p[H] = 6.5). In *E. chrysanthemi*, the ferric chrysobactin complexes are not shuttled through the FepA receptor (enterobactin transporter) but rather use their specific outer-membrane receptor Fct.[88] This bacterium is also able to take advantage of enterobactin as an exosiderophore, and the trafficking of the corresponding ferric complexes exclusively takes place via a related FepA receptor. Last, it was reported that only the ferric tris(chelate) complex of chrysobactin exhibited an optical activity, while the bis(chelate) is an achiral species.[19] Taking into account this information and assuming low concentrations of the tris(chelate) support the fact that the Fct receptor most likely binds the ferric bis(chrysobactin) complex. The achiral nature of this ferric species and the high homology of Fct (36%) with FoxA,[15] the specific transporter of ferrioxamine B, provide additional information and suggest comparable recognition properties, which may involve the terminal ammonium function as the structural key.[89,69b]

We have also examined the formation and dissociation kinetics of the ferric chrysobactin complexes in order to unravel the uptake and release mechanisms. The formation kinetics conducted under acidic conditions revealed that both CbH_4^+ and CbH_3 were involved with either $Fe(OH)^{2+}$ or $Fe_2(OH)_2^{2+}$. Regardless, the ferric species involved, CbH_3, was found to be 1 order of magnitude more reactive than CbH_4^+ mainly because of the presence of a neighboring carboxylate function, which assists the uptake of iron through electrostatic interactions and thus accelerates the formation. The acid-promoted dissociations of the ferric mono-, bis-, and tris(chrysobactin) complexes were also thoroughly examined and discussed. Our kinetic data revealed that, for the three ferric complexes, a single protonation was sufficient to trigger the dissociation of a chrysobactin molecule. Surprisingly, the release of chrysobactin from $FeCbH^+$ proceeds in a two-step process, while a monophasic mechanism was evidenced for ligand dissociation from $FeCb_3H_3^{3-}$ and $FeCb_2H_2^{2-}$. A ferric kinetic intermediate with a salicylate-type bonding was characterized by spectrophotometric data and explains this peculiar kinetic behavior. This intermediate then dissociates in the second rate-determining step, liberating free chrysobactin and iron(III).

It will be of importance to broaden our knowledge on the recognition mechanism of ferric chrysobactin complexes by Fct in *E. chrysanthemi*. Biochemical investigations under these directions are currently in progress.

Acknowledgment. This work has been supported by the Centre National de la Recherche Scientifique (UMR 7177). V.T. thanks the CNRS for a postdoctoral fellowship. D.E. is a researcher from the Centre National de la Recherche Scientifique.

Supporting Information Available: Pseudo-first-order rate constants of $FeCbH_2^{2+}$ formation (Table S1), chemical structure of achromobactin (Figure S1), ESI-MS spectra of the free chrysobactin (Figure S2) and of the ferric chrysobactin (Figure S3) complexes, ferric potentiometric titration curve of the free chrysobactin (Figure S4), distribution diagrams of the protonated species of chrysobactin (Figure S5), visible spectra recorded during spectrophotometric titration of chrysobactin with iron(III) at fixed p[H] = 2.00 (Figure S6), experimental kinetic data for the formation of the ferric chrysobactin complexes (Figure S7), experimental kinetic data for the acid-promoted dissociation of the ferric chrysobactin complexes (Figures S8−S11), distribution diagrams of the ferric chrysobactin complexes (Figure S12), and calculated structure of CbH_2^- species (Figure S13). This material is available free of charge via the Internet at http://pubs.acs.org.

IC801143E

(87) (a) Buckingham, D. A.; Clark, C. R.; Weller, M. G.; Gainsford, G. J. *J. Chem. Soc., Chem. Commun.* **1982**, 779–781. (b) Cohen, S. M.; Meyer, M.; Raymond, K. N. *J. Am. Chem. Soc.* **1998**, *120*, 6277–6286. (c) Cohen, S. M.; Raymond, K. N. *Inorg. Chem.* **2000**, *39*, 3624–3631.

(88) Persmark, M.; Expert, D.; Neilands, J. B. *J. Bacteriol.* **1992**, *174*, 4783–4789.

(89) Clarke, T. E.; Tari, L. W.; Vogel, H. J. *Curr. Top. Med. Chem.* **2001**, *1*, 7–30.